Biosensors and Bioelectronics 128 (2019) 104–112

Contents lists available at ScienceDirect

Biosensors and Bioelectronics

journal homepage: www.elsevier.com/locate/bios

Proximity recognition and polymerase-powered DNA walker for one-step and amplified electrochemical protein analysis

Zhiqiang Chen[a], Chao Wang[b], Lijie Hao[a], Rui Gao[a], Fang Li[b], Shufeng Liu[a,*]

[a] Key Laboratory of Optic-electric Sensing and Analytical Chemistry for Life Science, Ministry of Education; Shandong Key Laboratory of Biochemical Analysis, College of Chemistry and Molecular Engineering, Qingdao University of Science and Technology, No. 53, Rd., Zhengzhou, Qingdao 266042, China
[b] College of Marine Science and Biological Engineering, Qingdao University of Science and Technology, No. 53, Rd. Zhengzhou, Qingdao, Shandong 266042, China

ARTICLE INFO

Keywords:
Electrochemical biosensor
Protein analysis
Proximity recognition
DNA walker

ABSTRACT

The development of simple, flexible, cost-effective and sensitive electrochemical methods for protein analysis is of very importance for its potential application in disease diagnosis and biomedicine research. Herein, a new protein binding-induced proximity recognition and polymerase-powered DNA walker strategy was proposed for one-step and sensitive electrochemical quantification of proteins. Two DNA probes were designed with a hairpin-like one immobilized on the electrode and another one used as a DNA walker strand. The protein binding with the recognition elements labeled on these two probes brought their proximity hybridization, accompanied with the annealing of a redox probe-labeled primer strand on the opened immobilization probe. The DNA polymerization of primer strand in the presence of DNA polymerase induced the release of the DNA walker strand, which then walked to the adjacent immobilization probe for the proximity hybridization and progressive polymerase-powered DNA walker operation again. This induced the electrochemical signal reporting and amplifying toward protein quantification. The sensitive and selective detection toward proteins was achieved with the detection limits toward anti-dig antibody and streptavidin as 80 and 16 pM, respectively. Thus, the current study offers a simple, generic, one-step and amplified detection strategy for electrochemical protein quantification.

1. Introduction

With the role unveiling of more and more protein biomarkers in many important life processes and disease occurrence and development, accurate protein quantification by simple, cost-effective and point-of-care approaches is highly pursued to accommodate for disease diagnosis and biomedicine (Rifai et al., 2006; Borrebaeck, 2017; Jayanthi et al., 2017; Wu and Qu, 2015; Chandra, 2016). Till now, various techniques have been well explored toward the analysis of different proteins. The typical detection techniques include fluorescence, electrochemistry, electroluminescence, photoelectrochemistry, surface-enhanced raman scattering, etc (Chinen et al., 2015; Guarrotxena and Bazan, 2014; Zhang et al., 2017). Among them, electrochemical method possesses some inherent advantages such as simple instrumentation, signal stability, flexible operation and easy to integration and miniaturization (Wang, 2006; Mahshid et al., 2015). Nanomaterial or enzyme-based signal amplification strategies have been widely employed to improve the detection sensitivity toward protein analysis, as revealed in some recent references (Kerman et al., 2008; Wen et al., 2017; Shen et al., 2014; Toh et al., 2015; Huang et al., 2017). But they usually suffer from the multi-step, washing or reagent-intensive processes, especially in the case of electrochemical detection. Also, the preparation, purification and modification of nanomaterials further complicate the assay and even may bring some side effects on the detection performance such as reproducibility and stability. Alternatively, DNA-based signal amplification has been increasingly developed as a powerful and attractive means for protein analysis owing to its predictability and programmability of structure, facile synthesis and excellent amplification ability of DNA (Porchetta et al., 2018; Ren et al., 2015; Ferapontova, 2018). For example rolling circle amplification (RCA), polymerase chain reaction (PCR), strand displacement amplification (SDA), and hybridization chain reaction (HCR), etc. have been well incorporated into the fabrication of amplified protein biosensor (Robinson et al., 2016; Fredriksson et al., 2002; Yang et al., 2007; Huang et al., 2015; Li et al., 2015; Zhang et al., 2012). Although the detection sensitivity is attractive, they are often confronted with the relatively complex operation or design procedures, or even false-positive output (Borst et al., 2004; Craw and Balachandran, 2012; Zhang

* Corresponding author.
E-mail address: sliu@qust.edu.cn (S. Liu).

https://doi.org/10.1016/j.bios.2018.12.053
Received 9 October 2018; Received in revised form 27 December 2018; Accepted 28 December 2018
Available online 09 January 2019
0956-5663/

et al., 2013a, 2013b; Zhao et al., 2015).

Recently, DNA walker-based signal amplification has attracted substantial attention for building up sensitive and selective biosensors (Li et al., 2017; Wang et al., 2015; Qu et al., 2017; Yang et al., 2016a). DNA walkers can be regarded as a type of molecular machine, which usually moves progressively across the designed track based on a strand displacement cascade or nuclease-mediated DNA hydrolysis mechanism (Omabegho et al., 2009; Wickham et al., 2012; Jung et al., 2016; Yin et al., 2004). It can be also exploited for protein analysis with the aid of suitable nucleic acid-based protein recognition or conversion strategies (Zhu et al., 2018; Jiang et al., 2017; He et al., 2017; Zhang et al., 2014). The protein binding-induced DNA proximity recognition could be considered as a superior protein conversion strategy, which could enhance the detection selectivity and sensitivity owing to its dual or multiply recognition between protein and recognition elements labeled on the DNA (Wen and Ju, 2016; Yang et al., 2016b; Ranallo et al., 2017; Hu et al., 2014; Zhang et al., 2007, 2013b). Although DNA walker-based protein analysis has made great progress during the past years, most of reported strategies are involved into the co-immobilization of two or more different kinds of DNA strands or legs on the nanoparticle or biosensor surface (Omabegho et al., 2009; Jung et al., 2017; Li et al., 2018; Chen et al., 2017). The protein binding triggers the communication between these immobilized DNA strands for signal generation and amplification. Thus, the rational control of these different DNA strands on the surface is very crucial for the ultimate biosensor performance. In other word, the detection performance such as reproducibility and sensitivity would be easily influenced by the assembly behaviors of these DNA probes, which are relatively difficult to optimize. Also, the moving principle for current DNA walker is restricted to the toehold-mediated strand displacement or nucleic endonuclease or exonuclease-powered strategies (Yang et al., 2016a; Qu et al., 2017). Furthermore, they are more preferential for fluorescence detection. Thus, the development of new DNA walker-based protein analysis strategy with the simple, cost-effective, highly sensitive and selective attributes would be highly desirable for its potential diagnosis applications and even for basic research in biomedicine.

Herein, a new proximity recognition and cascade polymerase-powered DNA walker strategy was proposed for one-step and amplified electrochemical protein detection. Two DNA probes (P1 and P2) were designed and both were labeled with protein recognition elements. P1 had a hairpin-like structure and was immobilized on the electrode surface by an Au-S interaction. P2 was used as a DNA walker strand, which contained the complementary sequence with the loop region of P1 and numerous thymine (T) bases. The protein binding induced the proximity hybridization between P2 and P1 for the P1 opening. Then, the redox probe-labeled DNA primer strand (P3) could anneal with the P1 stem for the electrochemical signal generation. The DNA polymerization from 3′-terminus of P3 in the presence of DNA polymerase along the P1 template liberated the P2 strand, which could move to the adjacent P1 strand and induce again the proximity hybridization between P2 and P1 for the successive signal amplification toward protein recognition event. Different from most of reported DNA walker-based protein analysis strategy, the current proximity recognition and cascade polymerase-powered DNA walker strategy was only involved into the immobilization of one DNA strand on the electrode surface. Also, the whole protein recognition and amplification process could be accomplished by a simple one-step mixing operation. The anti-dig antibody and streptavidin were used as model proteins to demonstrate the detection capabilities and universality of current strategy.

2. Experimental section

2.1. Chemicals and materials

Bst DNA polymerase (Large Fragment) was purchased from New England Biolabs Inc. (Ipswich, MA, USA). Deoxyribonucleoside 5′-triphosphate (dNTPs) mixture, tris (2-carboxyethyl) phosphine hydrochloride (TCEP) and fetal calf serum were purchased from Sangon Biotech Co., Ltd. (Shanghai, China). Human serum sample from healthy donor was friendly provided by Qingdao Central Hospital (Qingdao, China). 6-Mercapto-1-hexanol (MCH), streptavidin (STA), thrombin and sheep polyclonal anti-digoxigenin antibody (anti-dig antibody) were obtained from Sigma-Aldrich (St. Louis, MO). Bovine serum albumin (BSA) and hemoglobin were supplied by Dingguo Biotech. Co., Ltd. (Beijing, China). The HPLC-purified DNA sequences were synthesized by Sangon Biotech. Co., Ltd. (Shanghai, China) and shown in Table S1. All other reagents were of analytical grade without further purification. All solutions were prepared with deionized water obtained from a Milli-Q water purification system (Millipore Corp., Bedford, MA, USA) with a resistivity of 18.2 MΩ cm.

2.2. DNA immobilization on the electrode surface

The gold electrode (2 mm diameter) was treated according to the previous reported procedures (Liu et al., 2017). Before use, all DNA sequences were heated to 90 °C for 5 min and then allowed to cool to room temperature for at least 2 h. The immobilization of a hairpin-like DNA probe (dig-P1 or biotin-P1) was operated by incubating the clean electrodes into 0.5 μM P1 of 10 mM PBS buffer (50 μL, 0.2 M NaCl, 10 mM TCEP, pH 7.4) for overnight at room temperature. After washing with 10 mM PBS buffer (pH 7.4, 0.2 M NaCl), the resulting electrode was further treated with 1 mM MCH solution for 1 h to remove any non-specific adsorbed DNAs.

2.3. Protein detection by proximity recognition and polymerase-powered DNA walker

Except specifically indicated, the protein detection was performed by incubating the P1 modified electrode into 10 mM PBS buffer (pH 7.4, 0.2 M NaCl, 20 mM $MgCl_2$) containing 50 nM P2, 0.5 μM P3, 0.16 U/μL Bst polymerase, 200 μM dNTPs and various concentrations of protein for 90 min at room temperature. The P1 and P2 were labeled with the respective recognition elements (dig for anti-dig antibody and biotin for streptavidin). After washing with 10 mM PBS (pH 7.4, 0.2 M NaCl), the electrode was ready for electrochemical measurement.

2.4. Electrochemical characterizations

Electrochemical measurements were performed on a CHI 660D electrochemical workstation (CH Instruments, Shanghai, China) at room temperature by using a three-electrode system. For anti-dig antibody analysis, the differential pulse voltammetry (DPV) and cyclic voltammetry (CV) were recorded in 10 mM PBS buffer (pH 7.4, 0.2 M KNO_3). The square wave voltammetry (SWV) and CV tests were used for streptavidin analysis and conducted in 10 mM Tris-HCl buffer (pH 7.4, 0.1 M NaCl). The electrochemical impedance spectroscopy (EIS) experiments were measured by using 5 mM $[Fe(CN)_6]^{3-/4-}$ in 10 mM PBS buffer (pH 7.4, 1 M KCl) with the frequency range of 0.1 Hz to 10 kHz. Before electrochemical measurements, the electrolyte solution should be thoroughly purged with high-purity nitrogen for approximately 20 min to avoid the interference from the reduction of oxygen.

3. Results and discussions

3.1. Protein detection principle by proximity recognition and polymerase-powered DNA walker

The detection principle toward protein was illustrated in Scheme 1. The anti-dig antibody was chosen as a model protein herein. Two DNA probes (P1 and P2) were designed and each was labeled with a protein recognition element (herein digoxigenin, abbreviated as dig) at the termini. The P1 strand with a hairpin-like structure was immobilized on

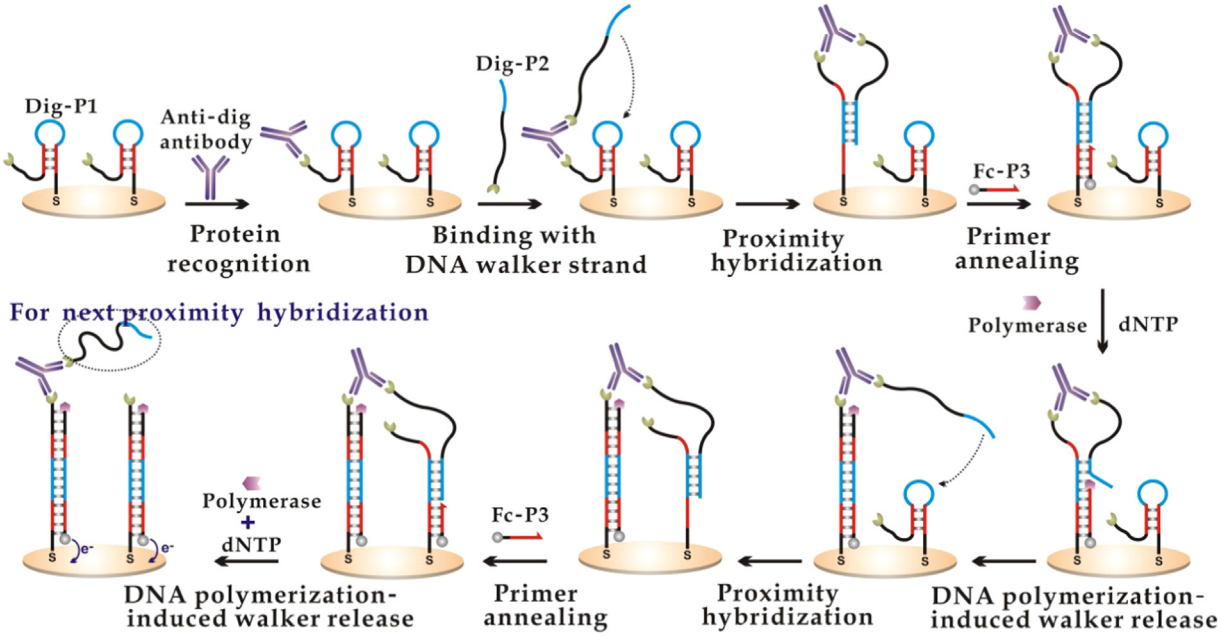

Scheme 1. Schematic illustration of the detection principle for anti-dig antibody.

the electrode surface by an Au-S interaction. The P2 strand contained the complementary base sequences with the loop region of the P1, and was used as a swing arm for DNA walker operation. Also, both P1 and P2 contained numerous thymidine (T) bases to maintain the freedom for proximity recognition. The base sequences of the redox probe-labeled primer (P3) were complementary with the base sequences at the 3′-terminus of P1, but which were caged in the stem region of P1. Herein, the P3 strand was used as both a signal reporter and primer strand. In the presence of anti-dig antibody, the protein binding with the recognition elements labeled on the probes (P1 and P2) brought their proximity hybridization owing to the increased local concentrations (Zhang et al., 2013). Then the stem-loop structure of P1 was opened, and the base sequences at the stem region of 3′-terminus of P1 were exposed, which could then hybridize with the P3. The redox probe labeled on the P3 strand was thus introduced on the electrode to indicate the electrochemical response. In the presence of polymerase and dNTPs, the DNA polymerization from the 3′-terminus of P3 along the P1 template induced the release of the swing arm of P2, which then moved to the adjacent P1 for proximity hybridization, accompanied with the P1 opening for the further annealing with P3 again. The successive polymerase-powered DNA walker operation contributed to the amplified electrochemical response toward the analyzed protein. In the absence of target protein, such a proximity hybridization process between P1 and P2 could not occur, and then the P3 strand could not autonomously anneal with the caged P1 for the generation of electrochemical signal toward the protein. Thus, such dynamic process for proximity recognition and polymerase-powered DNA walker could occur autonomously on the electrode surface once the analyzed protein was present in the sensing system. The recorded electrochemical signal after dynamic process was directly used for protein quantification.

3.2. Detection feasibility toward anti-dig antibody

The detection feasibility toward anti-dig antibody was then verified by differential pulse voltammetry (DPV) experiments. DPV measurement could alleviate the background current effect to a large extent, especially after baseline correction. The P3 itself could not hybridize with the immobilized P1 for the signal generation, which could be confirmed by acquisition of only a very weak current response (curve a in Fig. 1A). Furthermore, a small background electrochemical response of ferrocene could be only obtained in the case of no anti-dig antibody (curve b in Fig. 1A). This indicated that the P2 itself could not open the immobilized P1 by direct hybridization and thus the P3 could not anneal with P1 for signal generation. The addition of anti-dig antibody gave an obvious electrochemical response at about 0.215 V related with the reduction of ferrocene (curve d in Fig. 1A), which could be attributed to the protein binding-induced proximity hybridization between P1 and P2, accompanied with the annealing of P3 with the opened P1 for signal generation. Also, the 3′-terminus of P3 could be elongated across the P1 template in the presence of DNA polymerase, inducing the liberation of P2 to participate into the successive proximity recognition with the adjacent P1 for signal amplification. This point could be verified according to the observed current decrease in the absence of DNA polymerase (curve c in Fig. 1A). The above processes were also followed by cyclic voltammetry (CV) experiments (Fig. 1B). A pair of obvious redox peaks of ferrocene (oxidation potential of about 0.25 V and reduction potential of about 0.21 V) could be observed in the presence of anti-dig antibody (curve d in Fig. 1B). Such redox responses of ferrocene were evidently decreased in the absence of DNA polymerase (curve c in Fig. 1B), and the control experiments conducted in the absence of anti-dig antibody or only by P3 gave almost indiscernible electrochemical responses (curves a and b in Fig. 1B). These experiments demonstrated the detection feasibility toward anti-dig antibody. To ascertain that the proximity recognition and polymerase-powered DNA walker process depends on simultaneous binding of anti-dig antibody with both dig-labeled probes (P1 and P2), we used the unlabeled P1 or P2 as substitute. Fig. 1C showed that omission of dig whether for P1 or P2 gave no evident electrochemical responses, confirming the necessity for protein binding with two probes. We also validated the detection feasibility of this strategy against anti-dig antibody by using fluorescent method (Fig. S1). Herein, the gold electrode was replaced by gold nanoparticles (AuNPs) and the FAM-labeled P3 was used as a primer strand and fluorescence signal reporter (Experimental details shown in supporting information). The sole FAM-P3 in the solution showed a strong fluorescence response (curve a). The fluorescence signal was significantly reduced when the anti-dig antibody was added in the whole sensing system (curve d). However, in the absence of anti-dig antibody, the fluorescence response of FAM-P3 was only slightly decreased (curve b). The fluorescence signal decrease in the absence of Bst polymerase was evidently smaller than that for the intact sensing

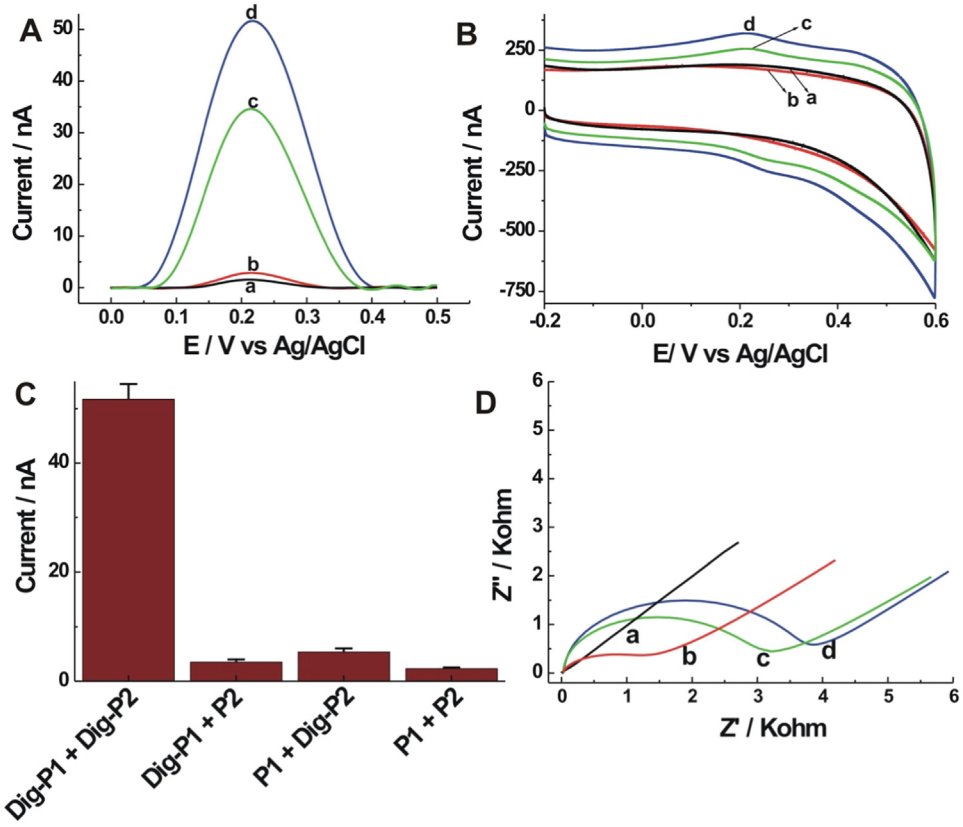

Fig. 1. DPV (A) and CV (B) responses toward 0 (b) and 100 nM anti-dig antibody (d). The control experiments were for Fc-P3 only (a) or no DNA polymerase (c) in the sensing system. (C) The use of P1 or P2 with no dig label as an alternative for the response toward 100 nM anti-dig antibody. The error bars were based on three repetitive experiments (D) EIS characterization toward different modified electrodes (a, bare electrode; b, P1 immobilized; c, after MCH assembly; d, after incubation with 100 nM anti-dig antibody in the sensing system). Other conditions: P2 (100 nM), P3 (500 nM), incubation time (2 h).

system (curve c). The fluorescence experiments further evidenced the detection principle for protein.

The electrochemical impedance spectroscopy (EIS) method was further employed to follow the biosensor fabrication process (Ohno et al., 2013). The bare gold electrode showed an almost straight line, suggesting a diffusion-controlled charge transfer process (curve a in Fig. 1D). The assembly of P1 on the electrode surface induced an increased charge transfer resistances (Rct) of 1120 Ω (curve b in Fig. 1D). This indicated the diffusion inhibition of $[Fe(CN)_6]^{3-/4-}$ to the electrode surface by the introduced negative charge of nucleic acid skeleton. The Rct value was increased to be 3150 Ω (curve c in Fig. 1D) after post-treatment of MCH. Thus, the relatively dense monolayer of MCH monolayer made the access of $[Fe(CN)_6]^{3-/4-}$ toward electrode surface more difficult. After protein binding-induced proximity recognition and polymerase-powered DNA walker operation, the steric hindrance or electrostatic repellence of the resulted electrode toward $[Fe(CN)_6]^{3-/4-}$ diffusion enhanced, inducing a Rct value to be 3800 Ω (curve d in Fig. 1D). In the absence of target protein, no evident change of Rct value could be observed compared with the P1 and MCH modified electrode (data no shown), indicating that the P1 could be not autonomously opened by P2 for further polymerase-powered DNA walker operation. The corresponding CV characterizations were also shown in Fig. S2. The redox peak current of $[Fe(CN)_6]^{3-/4-}$ decreased and the peak to peak potential increased following each assembly process. According to the Randles-Sevcik equation, $I_{pc} = (2.69\times10^5)n^{3/2}AD^{1/2}C^*v^{1/2}$ (I_{pc}, reduction peak current; n, electron transfer number; A, electroactive surface area; C, concentration; v, scan rate; D diffusion coefficient), it can be concluded that, when other parameters are unchanged, the value of ($AD^{1/2}$) is in proportional to the I_{pc} value. The I_{pc} values were decreased with the stepwise modification process on the electrode surface, reflecting the corresponding decreased ($AD^{1/2}$) values after different modifications. It further indicated that the $Fe(CN)_6^{3-/4-}$ could not approach to the modified electrode as easily as to the bare Au electrode, and it became more and more difficult with the stepwise modification process (Xu et al., 2006).

3.3. Optimization of corresponding experimental conditions

On the basis of detection feasibility for anti-dig antibody, the corresponding experimental conditions were optimized for the performance improvement. Firstly, the immobilization concentration of P1 was optimized. As shown in Fig. 2A, the background signal changed only slightly at the studied P1 concentrations. However, the electrochemical signal toward 100 nM anti-dig antibody responded distinctly with the P1 concentration, and it was firstly increased and then decreased after the concentration of P1 over 0.5 μM. An increased immobilization amount of P1 on the electrode would contribute the enhanced electrochemical response. However, the further increased assembly amount of P1 would be not benefit for the protein binding-induced proximity recognition and polymerase-powered DNA walker operation owing to the possible steric hindrance effect. Thus, 0.5 μM of P1 was chosen as the optimized immobilization concentration considering the maximum values of both absolute response and signal to background ratio. Also, the detection performance would be influenced by the hybridized base number between the P1 and P2 (Fig. 2B). Less hybridized base number would limit the protein binding-induced proximity hybridization reaction, resulting in only a low signal response toward anti-dig antibody. When the hybridized base number was over 17, the background response became evident, indicating the direct hybridization between the P2 and P1 occurred for the P1 opening even in the absence of anti-dig antibody. It could be also found that, when the hybridized base number reached 21, the background signal was very close to the signal response toward anti-dig antibody. In our design, the hybridized base number of 15 between the P1 and P2 could realize a higher signal to background ratio and was thus determined as an optimized value. Then, we optimized the P2 concentration (Fig. 2C). The electrochemical response toward anti-dig antibody increased with the increase of P2 concentration and the tendency became slowly after

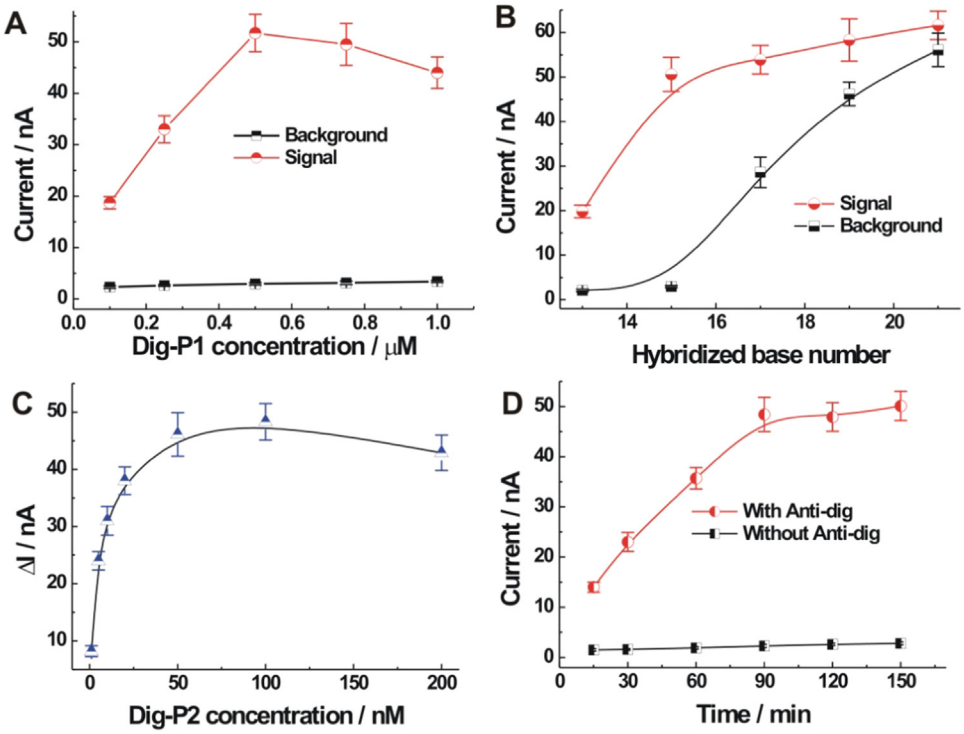

Fig. 2. (A) Optimization of immobilization concentration of P1. (B) Optimization of hybridized base number between P1 and P2. A series of P2 strands were used with 13, 15, 17, 19 and 21 complementary bases with the P1. (C) Optimization of dig-P2 concentration. The used dig-P2 concentration includes 1, 5, 10, 20, 50, 100 and 200 nM. (D) Optimization of reaction time. The error bars were based on three repetitive experiments.

the concentration of P2 over 50 nM. When the P2 concentration is further increased to be over 100 nM, a decreased electrochemical response toward anti-dig antibody could be observed. It might be caused that too much P2 depleted the recognition site of anti-dig antibody and shielded the recognition of anti-dig antibody with the immobilized P1 to some extent. Also, considering that relatively low P2 concentration might favor to probe low amount of target protein, the P2 concentration of 50 nM was used for further experiments. Finally, the effect of incubation time on the electrochemical response was studied (Fig. 2D). The signal response toward anti-dig antibody increased with the increasing incubation time and almost reached the saturation value after 90 min. Also, the background signal change was not obvious in the studied time range. Thus, an incubation time of 90 min was chosen for protein binding-induced proximity recognition and polymerase-powered DNA walker process in the following experiments.

3.4. Detection performance toward anti-dig antibody

The sensing performance of current strategy for anti-dig antibody was then explored and the titration experimental results were shown in Fig. 3A. The DPV peak current intensified as the protein concentration increased from 0 to 200 nM, showing a concentration-related response manner. The corresponding calibration curve was shown in Fig. 3B. The DPV peak current was in linear relationship with the anti-dig antibody concentration (0.3–5 nM), which was fitted by a regression equation of $I = 2.49 + 5.80\,C$ (I and C were for the current and target protein concentration, respectively) with a correlative coefficient of about 0.9910 (inset in Fig. 3B). A low detection limit of 80 pM was achieved based on 3σ method (defined as 3 times the standard deviation of the background response), which was superior or comparable with some reported methods (Table S2). The relative standard deviation (RSD) values for three concentrations of anti-dig antibody (0.5, 5 and 20 nM) were obtained as 8.57%, 6.8% and 7.3%, respectively, based on six repetitive measurements, suggesting an acceptable detection reproducibility.

As a comparison, the detection of anti-dig antibody was also executed in the absence of DNA polymerase. In this case, only protein binding-induced proximity recognition but no polymerase-powered DNA walker occurred. The electrochemical responses at different concentrations of anti-dig antibody were recorded in Fig. 3C. The DPV responses also intensified as the increasing anti-dig antibody concentration (0–250 nM). A linear plot could be also obtained for the DPV peak current versus anti-dig antibody concentration (1.5–20 nM) (Fig. 3D). The corresponding regression equation as I (current) $= 2.08 + 1.04\,C$ (concentration) could be given with a correlative coefficient of about 0.9915. The detection limit toward anti-dig antibody was only achieved as about 0.77 nM. Such a value was evidently higher than that by using DNA polymerase, confirmed the signal amplification ability of polymerase-powered DNA walker for protein detection.

3.5. Detection selectivity of fabricated electrochemical protein biosensor

The selective tests toward anti-dig antibody were shown in Fig. 4A and B. Only anti-dig antibody could give a distinct electrochemical response and some other nonspecific proteins resulted into almost the same values with the background response, suggesting the selective discrimination toward anti-dig antibody. The practical possibility of current biosensor in relatively complex matrix was further probed by conducting the detection of anti-dig antibody in the 5% diluted fetal calf serum (Fig. 4C) and human serum (Fig. S3A). Herein, a diluted serum was used as the assay medium for keeping the pH to approximate the buffer pH, and also reducing the possible effect of some biomolecules on the target protein to some extent. The corresponding calibration curves toward anti-dig antibody were shown in Fig. 4D and Fig. S3B. The statistical results for the detection of anti-dig antibody in diluted serum samples were also summarized in Table S3. The linear relationships for anti-dig antibody were obtained as I (current) $= 3.22 + 4.94\,C$ (concentration) in diluted fetal calf serum (0.5–5 nM) and I (current) $= 4.57 + 3.48\,C$ (concentration) in diluted human serum (0.5–8 nM). The detection limits toward anti-dig antibody were determined as 0.3 nM in diluted fetal calf serum and 0.18 nM in diluted human serum, which were higher than that in the buffer system. Thus, serum medium could exert some influences on the detection performance of protein. However, the current responses were still dependent

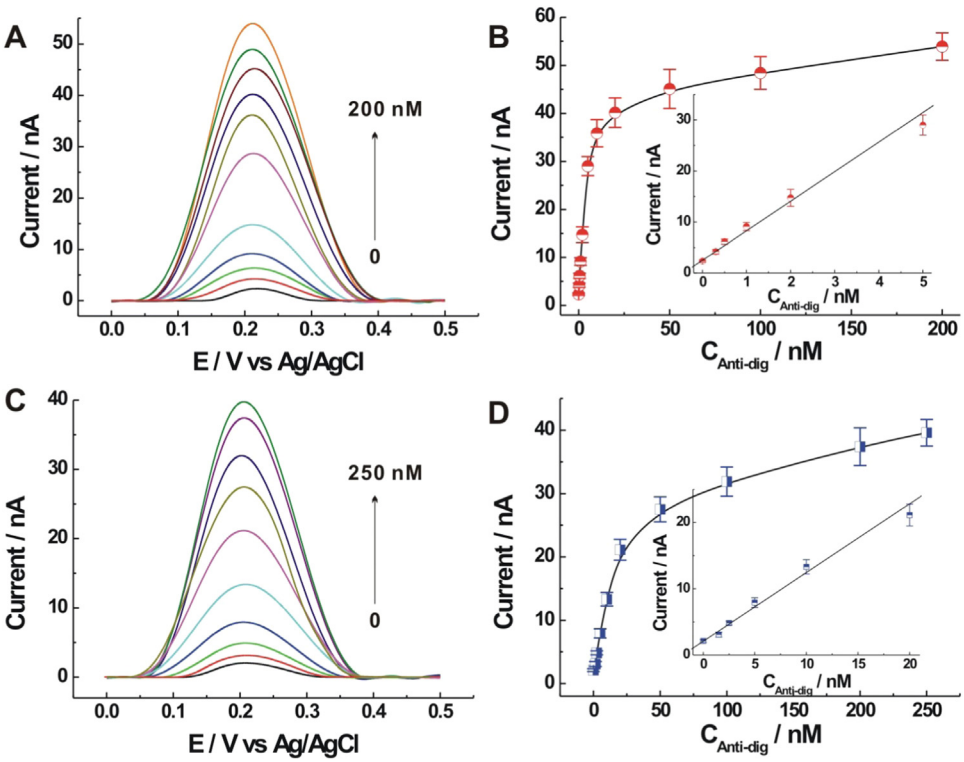

Fig. 3. (A) DPV responses toward different concentrations of anti-dig antibody (from bottom to up: 0, 0.3, 0.5, 1, 2, 5, 10, 20, 50, 100 and 200 nM). (B) Calibration curve between peak current and anti-dig antibody concentration. Inset shows the linear plot. (C) DPV responses toward different concentrations of anti-dig antibody in the absence of DNA polymerase (from bottom to up: 0, 1.5, 2.5, 5, 10, 20, 50, 100, 200, 250 nM). (D) Corresponding calibration curve and linear detection range (inset). The error bars were based on four repetitive experiments.

on the spiked protein concentrations in diluted serum. Such experiment showed the applicative potential of current method in relatively complex biological matrices to some extent.

3.6. Detection universality of fabricated electrochemical protein biosensor

The streptavidin was then employed as another multivalent model protein to demonstrate the detection feasibility and universality of the proposed strategy. The streptavidin can interact with the biotin or derivative with a high affinity, specificity and stability. It has been widely

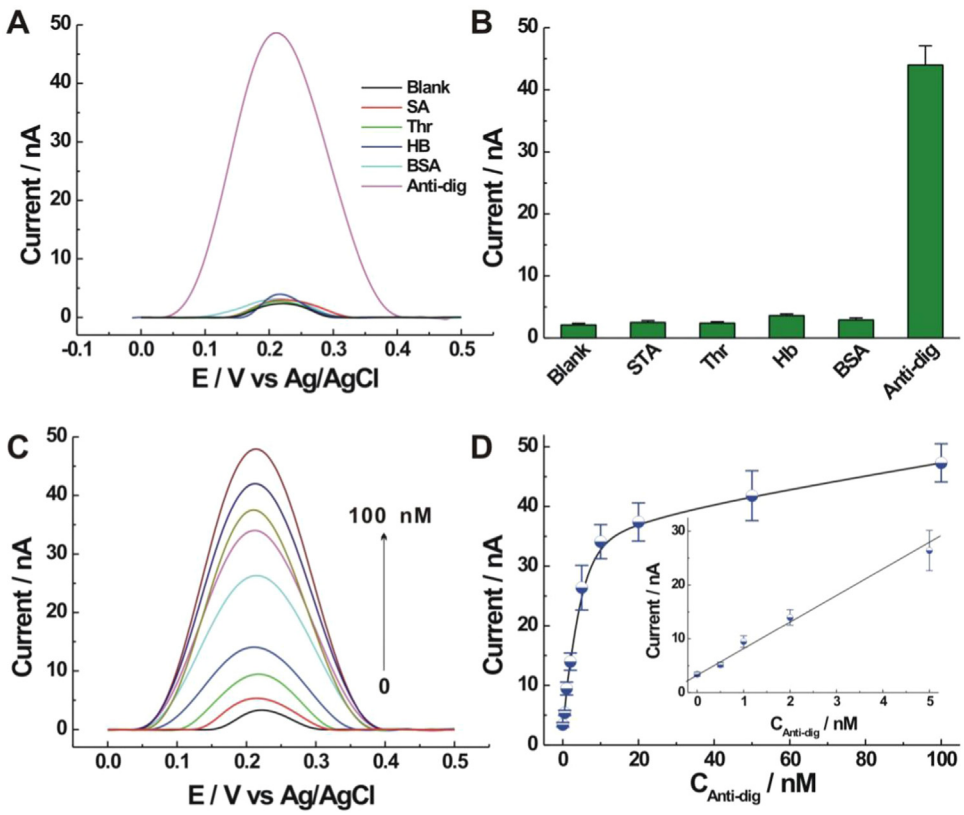

Fig. 4. DPV curves (A) and corresponding peak current values (B) by using 100 nM of different proteins: streptavidin (STA), thrombin (Thr), hemoglobin (Hb), bovine serum albumin (BSA) and anti-dig antibody. (C) DPV responses for different concentrations of anti-dig antibody spiked in 5% diluted fetal calf serum (from bottom to up: 0, 0.5, 1, 2, 5, 10, 20, 50, 100 nM). (D) Corresponding calibration curve and linear detection range (inset). The error bars were based on four repetitive experiments.

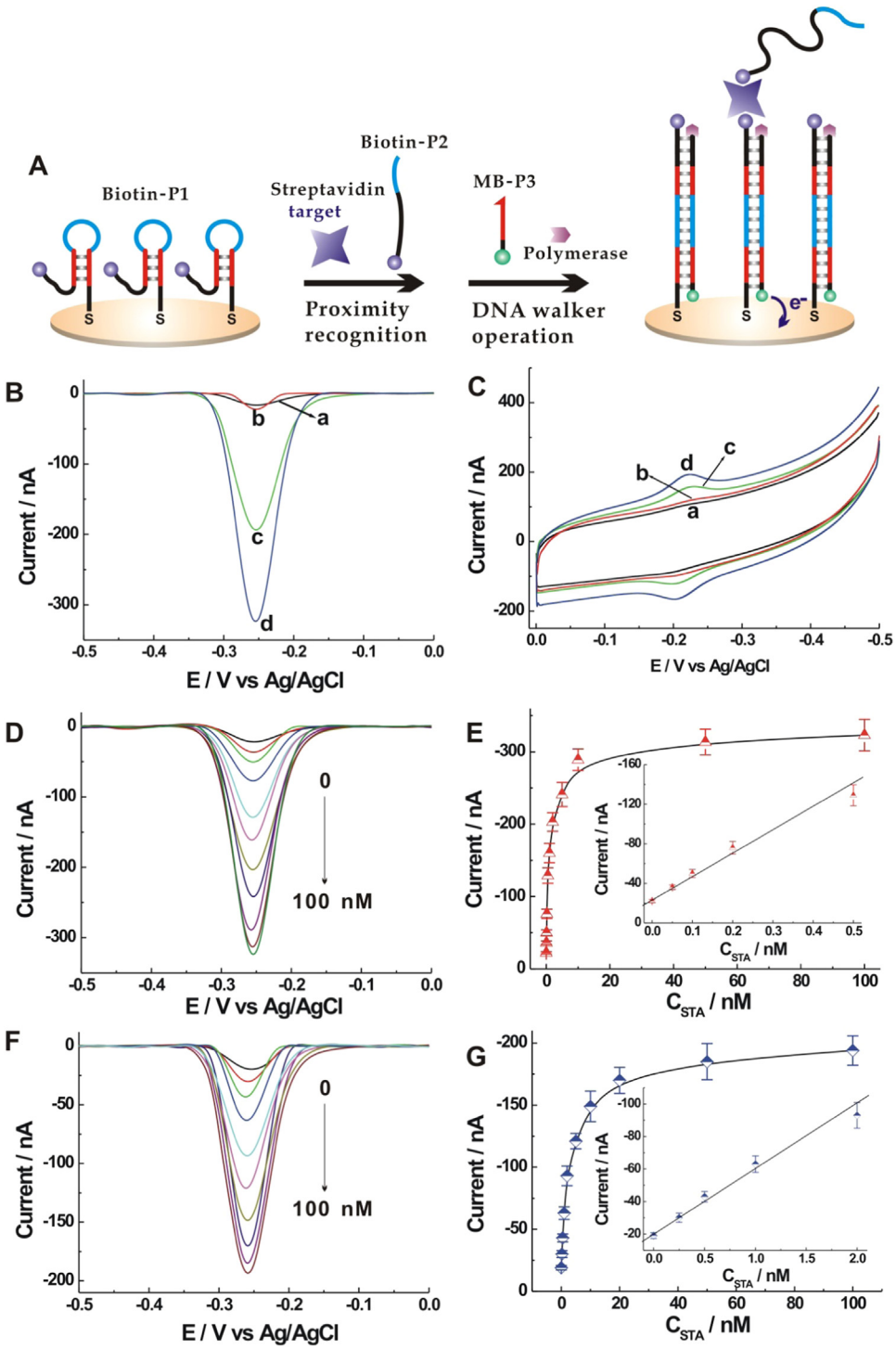

Fig. 5. (A) Schematic illustration for streptavidin detection. SWV (B) and CV (C) responses toward 0 (b) and (d) 100 nM streptavidin. The control experiments were for P3 strand only (a) or no DNA polymerase (c) in the sensing system. (D) SWV curves at different concentrations of streptavidin (from up to bottom: 0, 0.05, 0.1, 0.2, 0.5, 1, 2, 5, 10, 50, 100 nM). (E) Corresponding calibration curve and linear detection range (inset). (F) SWV responses at different concentrations of streptavidin in the absence of DNA polymerase (from up to bottom: 0, 0.25, 0.5, 1, 2, 5, 10, 20, 50, 100 nM). (G) Corresponding calibration curve and linear plot (inset). The error bars were based on four repetitive experiments.

applied as an ideal model system for biomolecular recognition and also for biosensor fabrication toward many diagnostic assays (Galarreta et al., 2011). The detection principle was almost the same with that for anti-dig antibody except that the recognition elements labeled on P1 and P2 were changed from dig into biotin moiety (Fig. 5A). Herein, another widely employed redox probe, methylene blue, was adopted as a label to indicate the electrochemical response toward protein since its better shelf life and performance (Kang et al., 2009). The corresponding experimental conditions were based on the above optimized values for anti-dig antibody detection. As shown in Fig. 5B, a distinct SWV response at about −0.255 V was observed in the presence of streptavidin, which was attributed to the electrochemical oxidation of methylene blue (curve d in Fig. 5B), whereas only a very small electrochemical response could be obtained in the absence of streptavidin (curve b in Fig. 5B). The control experiment by using P3 only could show a very small electrochemical response (curve a in Fig. 5B). The electrochemical response in case of no polymerase was also evidently lower (curve c in Fig. 5B), demonstrating again the polymerase-powered DNA walker strategy for signal amplification. The corresponding CV results were also recorded in Fig. 5C. Upon addition of streptavidin in the sensing system, an obvious pair of redox peaks of methylene blue could be obtained with an anodic and cathodic potential of −0.2 V and −0.22 V, respectively. The anodic and cathodic peak currents were 167 nA and 193 nA, respectively (curve d). The cyclic voltammogram

showed almost no redox responses in the absence of streptavidin (curve b) or by using P3 only as a control experiment (curve a). Also, in case of no polymerase, the redox response of methylene blue was evidently decreased (curve c). The CV results agreed well with the SWV results, verifying the detection feasibility toward streptavidin together. The corresponding control experiments were also designed to verify that the signal generation was originated from the concurrent binding of streptavidin with biotins labeled on P1 and P2 (Fig. S4). The selective detection toward streptavidin was revealed by comparing with other used non-specific proteins (Fig. S5). The corresponding electrochemical responses at different streptavidin concentrations were recorded in Fig. 5D. The electrochemical responses were highly related with the streptavidin concentrations. The SWV peak current demonstrated a linear relationship with the streptavidin concentration (0.05–0.5 nM) (Fig. 5E). The detection limit toward streptavidin was obtained as 16 pM. The detection reproducibility toward streptavidin was investigated with the RSD values of 8.2%, 8.38% and 5.3% for 0.1, 1 and 10 nM streptavidin, respectively (six repetitive measurements). Also, the responsive curves and corresponding calibration curve at different streptavidin concentrations were obtained in the absence of DNA polymerase as a comparison (Fig. 5F and G). In this case, only a detection limit of 0.12 nM could be achieved, verifying again the signal amplification effect of polymerase-powered DNA walker strategy for streptavidin detection.

We also conducted the streptavidin detection in the diluted fetal calf serum (Fig. S6). Electrochemical responses for different concentrations of streptavidin spiked in the diluted serum were comparable with that in the buffer (Fig. S6A). The detection results were also shown in Table S3. A linear detection range (0.1–0.5 nM) and a detection limit of 53 pM could be obtained for the streptavidin in the diluted serum (Fig. S6B). The recovery tests toward the spiked proteins (anti-dig antibody and streptavidin) in the diluted serum were also conducted. The recoveries were obtained from 92% to 112% with the relative standard deviation (RSD) between 5.6% and 9.6% (Table S4), which was acceptable for quantitative assays performed in relatively complex biological samples.

It should be noted that the current strategy mainly served for the detection of proteins with multiple binding motifs. Also, current detection sensitivity toward proteins might be further upgraded by combining some other signal amplification methods, for example nicking endonuclease/polymerase-dependent strand displacement amplification and nanomaterial or enzyme-based signal amplification.

4. Conclusions

In current research, a new protein binding-induced proximity recognition and cascade polymerase-powered DNA walker strategy was well developed for one-step and amplified electrochemical protein detection. The protein binding created the opportunity for the proximity hybridization between two designed recognition probes. The successive annealing of a redox probe-labeled DNA primer to trigger the polymerase-powered DNA walker contributed for the signal generation and amplification. The developed strategy for protein detection exhibited several distinct advantages: 1) it was only involved into the immobilization of one DNA substrate strand, whereas most of existing DNA walker strategy needed the co-immobilization of two or more different kinds of DNA strands, which increased the control difficulty for biosensor fabrication; 2) the whole assay process was easy to operate by only a one-step mixing operation; 3) it offered an enhanced detection specificity due to the affinity binding of two or more ligands for target protein; 4) DNA walker-based signal amplification endowed an attractive sensitivity with the low detection limit toward anti-dig antibody and streptavidin as 80 and 16 pM, respectively. Furthermore, the current proposed strategy should be also easily integrated with some other detection means for example fluorescence, electrochemiluminescence, etc. Thus, the current strategy provides an attractive avenue for generic and sensitive protein biosensor fabrication, and would also enlighten the development of more protein or DNA walkers or machines to serve for disease diagnosis and clinical biomedicine.

CRediT authorship contribution statement

Zhiqiang Chen: Methodology, Investigation, Writing - original draft. **Chao Wang:** Methodology, Visualization. **Lijie Hao:** Software, Data curation, Formal analysis. **Rui Gao:** Validation, Data curation. **Fang Li:** Supervision. **Shufeng Liu:** Conceptualization, Writing - review & editing, Supervision.

Acknowledgements

We acknowledged the finance supports from the National Natural Science Foundation of China (No. 21475072), the Natural Science Foundation of Shandong Province of China (Nos. JQ201704 and ZR2015JL007), the Key Research and Development Program of Shandong Province of China (2016GSF201208), and the Open Project from Fujian Provincial Key Laboratory of Ecology-Toxicological Effects & Control for Emerging Contaminants.

Appendix A. Supporting information

Supplementary data associated with this article can be found in the online version at https://doi.org/10.1016/j.bios.2018.12.053.

References

Borrebaeck, C.A.K., 2017. Nat. Rev. Cancer 17, 199–204.
Borst, A., Box, A.T.A., Fluit, A.C., 2004. Eur. J. Clin. Microbiol. Infect. Dis. 23, 289–299.
Chandra, P., 2016. Nanobiosensors for Personalized and Onsite Biomedical Diagnosis. The Institution of Engineering and Technology, London, UK.
Chen, J., Zuehlke, A., Deng, B., Peng, H., Hou, X., Zhang, H., 2017. Anal. Chem. 89, 12888–12895.
Chinen, A.B., Guan, C.M., Ferrer, J.R., Barnaby, S.N., Merkel, T.J., Mirkin, C.A., 2015. Chem. Rev. 115, 10530–10574.
Craw, P., Balachandran, W., 2012. Lab Chip 12, 2469–2486.
Ferapontova, E.E., 2018. Annu. Rev. Anal. Chem. 11, 197–218.
Fredriksson, S., Gullberg, M., Jarvius, J., Olsson, C., Pietras, K., Gústafsdóttir, S.M., Östman, A., Landegren, U., 2002. Nat. Biotechnol. 20, 473–477.
Galarreta, B.C., Norton, P.R., Lagugné-Labarthet, F., 2011. Langmuir 27, 1494–1498.
Guarrotxena, N., Bazan, G.C., 2014. Adv. Mater. 26, 1941–1946.
He, M.Q., Wang, K., Wang, W.J., Yu, Y.L., Wang, J.H., 2017. Anal. Chem. 89, 9292–9298.
Hu, J., Yu, Y., Brooks, J.C., Godwin, L.A., Somasundaram, S., Torabinejad, F., Kim, J., Shannon, C., Easley, C.J., 2014. J. Am. Chem. Soc. 136, 8467–8474.
Huang, X., Liu, Y., Yung, B., Xiong, Y., Chen, X., 2017. ACS Nano 11, 5238–5292.
Huang, Y., Liu, X., Huang, H., Qin, J., Zhang, L., Zhao, S., Chen, Z.F., Liang, H., 2015. Anal. Chem. 87, 8107–8114.
Jayanthi, V.S.A., Das, A.B., Saxena, U., 2017. Biosens. Bioelectron. 91, 15–23.
Jiang, X., Wang, H., Wang, H., Zhuo, Y., Yuan, R., Chai, Y., 2017. Anal. Chem. 89, 4280–4286.
Jung, C., Allen, P.B., Ellington, A.D., 2016. Nat. Nanotechnol. 11, 157–163.
Jung, C., Allen, P.B., Ellington, A.D., 2017. ACS Nano 11, 8047–8054.
Kang, D., Zuo, X., Yang, R., Xia, F., Plaxco, K.W., White, R.J., 2009. Anal. Chem. 81, 9109–9113.
Kerman, K., Saito, M., Yamamura, S., Takamura, Y., Tamiya, E., 2008. TrAC Trends Anal. Chem. 27, 585–592.
Li, F., Zhang, H., Wang, Z., Newbigging, A.M., Reid, M.S., Li, X.F., Le, X.C., 2015. Anal. Chem. 87, 274–292.
Li, W., Wang, L., Jiang, W., 2017. Chem. Commun. 53, 5527–5530.
Li, Y., Wang, G.A., Mason, S.D., Yang, X., Yu, Z., Tang, Y., Li, F., 2018. Chem. Sci. 9, 6434–6439.
Liu, S., Fang, L., Wang, Y., Wang, L., 2017. Anal. Chem. 89, 3108–3115.
Mahshid, S.S., Camiré, S., Ricci, F., Vallée-Bélisle, A., 2015. J. Am. Chem. Soc. 137, 15596–15599.
Ohno, R., Ohnuki, H., Wang, H., Yokoyama, T., Endo, H., Tsuya, D., Izumi, M., 2013. Biosens. Bioelectron. 40, 422–426.
Omabegho, T., Sha, R., Seeman, N.C., 2009. Science 324, 67–71.
Porchetta, A., Ippodrino, R., Marini, B., Caruso, A., Caccuri, F., Ricci, F., 2018. J. Am. Chem. Soc. 140, 947–953.
Qu, X., Zhu, D., Yao, G., Su, S., Chao, J., Liu, H., Zuo, X., Wang, L., Shi, J., Wang, L., Huang, W., Pei, H., Fan, C., 2017. Angew. Chem. Int. Ed. 56, 1855–1858.
Ranallo, S., Prévost-Tremblay, C., Idili, A., Vallée-Bélisle, A., Ricci, F., 2017. Nat. Commun. 8, 15150.
Ren, K., Wu, J., Yan, F., Zhang, Y., Ju, H., 2015. Biosens. Bioelectron. 66, 345–349.
Rifai, N., Gillette, M.A., Carr, S.A., 2006. Nat. Biotech. 24, 971–983.
Robinson, P.V., Tsai, C., de Groot, A.E., McKechnie, J.L., Bertozzi, C.R., 2016. J. Am.

Chem. Soc. 138, 10722–10725.
Shen, J., Li, Y., Gu, H., Xia, F., Zuo, X., 2014. Chem. Rev. 114, 7631–7677.
Toh, S.Y., Citartan, M., Gopinath, S.C.B., Tang, T.H., 2015. Biosens. Bioelectron. 64, 392–403.
Wang, J., 2006. Biosens. Bioelectron. 21, 1887–1892.
Wang, L., Deng, R., Li, J., 2015. Chem. Sci. 6, 6777–6782.
Wen, G., Ju, H., 2016. Anal. Chem. 88, 8339–8345.
Wen, W., Yan, X., Zhu, C., Du, D., Lin, Y., 2017. Anal. Chem. 89, 138–156.
Wickham, S.F.J., Bath, J., Katsuda, Y., Endo, M., Hidaka, K., Sugiyama, H., Turberfield, A.J., 2012. Nat. Nanotechnol. 2012 (7), 169–173.
Wu, L., Qu, X., 2015. Chem. Soc. Rev. 44, 2963–2997.
Xu, Y., Yang, L., Ye, X., He, P., Fang, Y., 2006. Electroanalysis 18, 873–881.
Yang, L., Fung, C.W., Cho, E.J., Ellington, A.D., 2007. Anal. Chem. 79, 3320–3329.
Yang, X., Tang, Y., Mason, S.D., Chen, J., Li, F., 2016a. ACS Nano 10, 2324–2330.
Yang, Z.H., Zhuo, Y., Yuan, R., Chai, Y.Q., 2016b. Anal. Chem. 88, 5189–5196.
Yin, P., Yan, H., Daniell, X.G., Turberfield, A.J., Reif, J.H., 2004. Angew. Chem. Int. Ed. 43, 4906–4911.
Zhang, B., Liu, B., Tang, D., Niessner, R., Chen, G., Knopp, D., 2012. Anal. Chem. 84, 5392–5399.
Zhang, C., Glaros, T., Manicke, N.E., 2017. J. Am. Chem. Soc. 139, 10996–10999.
Zhang, H., Li, F., Dever, B., Li, X.F., Le, X.C., 2013a. Chem. Rev. 113, 2812–2841.
Zhang, H., Li, F., Dever, B., Wang, C., Li, X.F., Le, X.C., 2013b. Angew. Chem., Int. Ed. 52, 10698–10705.
Zhang, Y.L., Huang, Y., Jiang, J.H., Shen, G.L., Yu, R.Q., 2007. J. Am. Chem. Soc. 129, 15448–15449.
Zhang, Z., Hejesen, C., Kjelstrup, M.B., Birkedal, V., Gothelf, K.V., 2014. J. Am. Chem. Soc. 136, 11115–11120.
Zhao, Y., Chen, F., Li, Q., Wang, L., Fan, C., 2015. Chem. Rev. 115, 12491–12545.
Zhu, C., Liu, M., Li, X., Zhang, X., Chen, J., 2018. Chem. Commun. 54, 10359–10362.